Two-Dimensional Fluorescence Correlation Spectroscopy. I. Analysis of Polynuclear Aromatic Hydrocarbons in Cyclohexane Solutions

Kenichi Nakashima,*,† Satoshi Yashuda,† Yukihiro Ozaki,‡ and Isao Noda§

Department of Chemistry, Faculty of Science and Engineering, Saga University, Saga 840-8502, Japan, Department of Chemistry, School of Science, Kwansei-Gakuin University, Uegahara, Nishinomiya 662-8501, Japan, and Miami Valley Laboratories, The Procter and Gamble Company, P.O. Box 538707, Cincinnati, Ohio 45253-8707

Received: November 5, 1999; In Final Form: June 20, 2000

Generalized two-dimensional (2D) correlation spectroscopy was applied to the analysis of fluorescence spectra of anthracene−phenanthrene (AN−PH) and anthracene−pyrene (AN−PY) mixtures in cyclohexane solutions. These aromatic hydrocarbons are commonly used fluorescence probes. They have fine-structured and well-characterized spectra suitable for investigating basic features of the 2D fluorescence correlation spectroscopy. The AN−PH pair was examined as an example in which the component spectra are not heavily overlapped, while the AN−PY pair is an example in which the component spectra are heavily overlapped. We used two types of perturbation to induce the intensity variations of fluorescence spectra: one is concentration change, and the other is excitation-wavelength change. Both perturbations gave a series of systematically varying spectra, which led to the development of clear synchronous and asynchronous maps. By using the 2D correlation maps thus obtained, the vibronic bands in the complicated fluorescence spectra of the mixture of the probes were successfully analyzed. This study demonstrates the usefulness and potentiality of the 2D correlation technique in the field of fluorescence spectroscopy.

1. Introduction

A concept of the two-dimensional (2D) correlation method was proposed by Noda in the field of infrared (IR) spectroscopy in 1986,[1] which is different from the double time-domain Fourier transform (FT) method used extensively in NMR. He employed a simple cross-correlation analysis to construct a pair of 2D IR correlation spectra. The principle of this method is to perturb a system by an external stimulation such as electric field or mechanical tension, followed by calculation of the correlation between the responses of bands arising from the dynamic reorganization of constituents of the system. This technique was shown to be useful for revealing spectral features which cannot readily be seen in the original spectra.[2,3] In the earlier stage of the development of 2D IR correlation spectroscopy, however, the perturbation was restricted to a stimulation which changes sinusoidally with a small amplitude. Because of this restriction, the 2D IR correlation spectroscopy was applied to a limited number of systems.

A more generally applicable 2D correlation spectroscopy was developed by the same author in 1993.[4] In this method the perturbation does not need to have a sinusoidal form, but can have an arbitrary and complex form. Moreover, a variety of stimulation, other than electric or mechanic stress, can be employed for inducing spectral intensity fluctuations. Such stimulation includes the variations of pressure, temperature, and chemical compositions. Owing to these advantages, the applications of generalized 2D IR correlation spectroscopy are rapidly increasing.[5−10]

In his first paper on the generalized 2D correlation spectroscopy, Noda suggested the extension of this technique to other spectral regions and spectral modes such as UV−vis, X-ray, and Raman.[4] It has already been extended to near-infrared (NIR) and Raman spectroscopy and has been shown to be of great use also in these applications.[11−22]

Fluorescence spectroscopy is a sensitive and selective tool to probe various systems such as solutions, colloids, organic and inorganic solids, and polymers.[23−25] Despite the usefulness, the analysis of fluorescence spectra is sometimes difficult, especially if they are complicated by a heavy overlap of the contributions from constituents of the system. To overcome this problem, several analysis techniques have been employed. Such techniques include factor analysis,[26−28] excitation−emission matrix type two-dimensional fluorescence analysis,[29,30] and extended cross correlation (XCC) analysis.[31−33] These techniques have been shown to be useful for analyzing complicated systems containing two or more components. However, an additional novel analysis technique, which is based on a very different principle, will also be useful. Therefore, we extend the 2D correlation method proposed by Noda[4] to the field of fluorescence spectroscopy. One of the major advantages of the generalized 2D correlation method, compared to the previous methods, is that asynchronous correlation maps can give information about the order of physical and chemical changes such as conformational changes of polymers and formation (or cleavage) of hydrogen bonds (see the literature[11−17] for details). This advantage has never been seen in the previous analysis methods, because they were developed mainly from the standpoint of analytical chemistry (i.e., that of component analysis). In fact, the 2D correlation method will be of great use in investigations in physical chemistry, as well.

* To whom correspondence should be sent.
† Saga University.
‡ Kwansei-Gakuin University.
§ The Procter and Gamble Co.

10.1021/jp9939165 CCC: $19.00
Published on Web 09/20/2000

It should be emphasized here that the present 2D fluorescence *correlation* spectroscopy is based on completely different principle from that of conventional *excitation−emission matrix* type 2D fluorescence spectroscopy.[29,30] Whereas the former shows the true correlation of the behaviors of fluorescence bands, the latter simply illustrates excitation and emission spectra simultaneously in two dimensions to show the dependence of fluorescence spectra on the excitation wavelength. The difference is clearly shown in the next section. The XCC technique proposed by Field's group[31−33] is also different from ours, although their method is based on correlation analysis. The XCC is a pattern recognition technique, and is similar to those based on principal component analysis. The correlation loci are plotted on a intensity−intensity plane.

The first application of 2D correlation method to fluorescence spectroscopy was reported by Roselli et al. to investigate metal-binding sites of proteins.[34] They analyzed the fluorescence from Yb^{3+} at two different binding sites of transferrin. The perturbation method used by Roselli et al. was to change excitation wavelength. There are several techniques other than excitation-wavelength change that cause the change of fluorescence intensity. It should greatly increase the usefulness and potentiality of 2D fluorescence correlation spectroscopy if we establish the applicability of such perturbation methods. In particular, the quenching technique and sensitization technique, which are exclusive to fluorescence spectroscopy, seem to be promising methods.

In a series of studies, we plan to try several approaches to 2D fluorescence correlation spectroscopy. In this first paper, we report the analysis of anthracene−phenanthrene and anthracene−pyrene mixtures in cyclohexane solutions by employing two perturbation methods: concentration change and excitation-wavelength change. In contrast to Yb^{3+} employed by Roselli et al., anthracene (AN), phenanthrene (PH), and pyrene (PY) are much more commonly used probes which have fine-structured and well-characterized fluorescence spectra. Therefore, these aromatic hydrocarbons seem to be more appropriate for investigating basic features of 2D fluorescence correlation spectroscopy.

2. Theoretical Background

The mathematical background for generalized 2D correlation spectroscopy has been given in the literature.[4] Here we focus on the description concerning its application to fluorescence spectroscopy. To obtain correlation maps, we have to apply some perturbation to the system, which causes intensity variations in fluorescence spectra. In the present treatments we employ two types of perturbations. One is to alter the concentrations of the components: we refer to this as *concentration perturbation*. This approach has already been employed for our earlier studies on polymer blends by Raman, NIR, or IR correlation spectroscopy.[21,22,35] The other is to vary an excitation wavelength: we refer to this as *excitation perturbation*.

Because the excitation perturbation is exclusive to 2D fluorescence correlation spectroscopy, it seems necessary to give a detailed explanation. Fluorescence intensity, $I_f(\lambda_f,\lambda_{ex},C)$, of a fluorophore in a dilute solution is generally expressed by

$$I_f(\lambda_f,\lambda_{ex},C) = I_{ex}(\lambda_{ex})\,\epsilon(\lambda_{ex})\,C\,\phi(\lambda_{ex}) \qquad (1)$$

where λ_{ex} and λ_f are the wavelengths of excitation light and fluorescence emission, respectively, $I_{ex}(\lambda_{ex})$ is the intensity of excitation light, $\epsilon(\lambda_{ex})$ is the extinction coefficient of the fluorophore, C is the concentration of the fluorophore, and $\phi(\lambda_{ex})$ is the fluorescence quantum yield. Equation 1 clearly shows that the fluorescence intensity is dependent on excitation wavelength, λ_{ex}, and concentration of the fluorophore, C. This is the basis for the excitation perturbation and the concentration perturbation. If we observe the fluorescence intensity at a fixed λ_{ex} by varying λ_f, we obtain a *fluorescence* spectrum. On the other hand, if we observe the fluorescence intensity at a fixed λ_f by varying λ_{ex}, we obtain an *excitation* spectrum.

In the excitation perturbation method, we observe fluorescence spectra of a sample (with fixed concentration) at a series of excitation wavelengths, $\lambda_{ex,m}$ ($m = 1 - N$). The fluorescence spectra thus obtained are expressed as $I_f(\lambda_f,\lambda_{ex,m})$. The synchronous and asynchronous 2D fluorescence correlation intensities, $\Phi(\lambda_{f1},\lambda_{f2})$ and $\Psi(\lambda_{f1},\lambda_{f2})$, become

$$\Phi(\lambda_{f1},\lambda_{f2}) + i\Psi(\lambda_{f1},\lambda_{f2}) = [\pi(\lambda_{ex,N} - \lambda_{ex,1})]^{-1} \int_0^\infty Y_1(\omega)Y_2^*(\omega)\mathrm{d}\omega \qquad (2)$$

where $Y_1(\omega)$ is the excitation-wavelength-domain Fourier transform of $I_f(\lambda_{f1},\lambda_{ex})$ and $Y_2^*(\omega)$ is the conjugate of the Fourier transform of $I_f(\lambda_{f2},\lambda_{ex})$. It is obvious from this formulation that the present 2D fluorescence correlation maps are completely different from conventional excitation−emission matrix type 2D fluorescence spectra, in which the fluorescence intensity, $I_f(\lambda_f,\lambda_{ex})$, is simply illustrated as a function of λ_f and λ_{ex}.

3. Experimental Section

PH and PY were purified by vacuum sublimation. AN (Tokyo Kasei Kogyo Co., Ltd.) was a zone-refined sample, and thus used without further purification. Cyclohexane (Dojin Kagaku Co., Ltd.) is a solvent for fluorescence spectroscopy, and was used as received.

The stock solution (10 μM) of each fluorophore was prepared with cyclohexane. Portions of the stock solutions were transferred into 10-mL volumetric flasks to give appropriate molar ratios of the fluorophores.

Fluorescence and excitation spectra were recorded on a Hitachi F-4000 spectrofluorometer. The fluorescence spectra were calibrated by the use of a standard tungsten lamp with a known color temperature. The excitation spectra were corrected by a conventional rhodamine B method.

The 2D correlation maps were generated with a software "2D Pocha" which was programmed at Kwansei-Gakuin University.

4. Results and Discussion

4.1. Anthracene−Phenanthrene Mixture. We employed the AN−PH pair as a model case where the fluorescence spectra are not heavily overlapped, so that the band assignment is relatively easy even by a conventional one-dimensional method. Figure 1 shows fluorescence spectra of AN and PH observed individually in cyclohexane solutions. It is well known that both AN and PH have fine-structured vibronic bands. For the convenience of the following discussion, the bands are denoted Hi (i = 1−5) for PH and Ai (i = 1−4) for AN. As seen in Figure 1, the bands H1, H2, H3, A3, and A4 are not significantly overlapped with any other bands. The locations of the bands are summarized in Table 1.

Figure 2 represents fluorescence spectra of the mixtures of AN and PH in cyclohexane solutions with varying molar concentrations of the probes. The band intensities of AN and PH are changed along with changes in their concentration. Using these spectra, we calculated synchronous and asynchronous maps for the system (Figure 3).

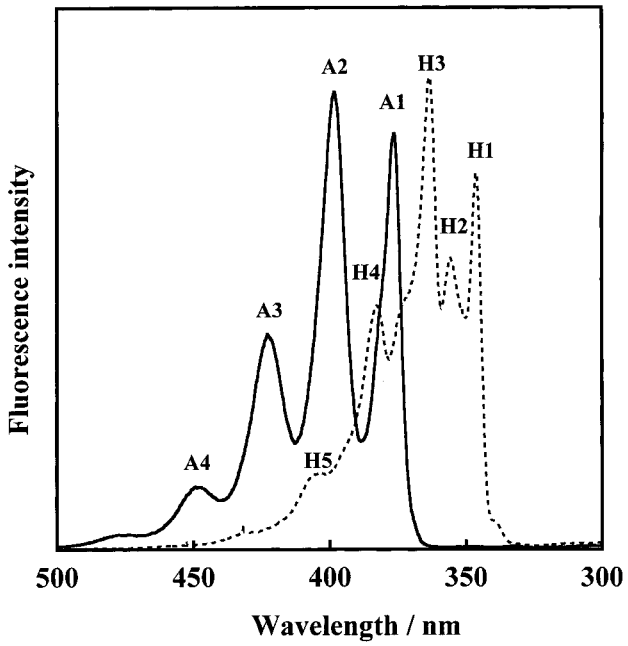

Figure 1. Fluorescence spectra of AN (—) and PH (···) in cyclohexane solutions. Concentrations: [AN] = 10 μM, [PH] = 10 μM. The samples are excited at 262 nm. Excitation and emission band-passes are 5 and 3 nm, respectively. The excitation wavelength, 262 nm, is selected in order that the fluorescence of both probes may become comparable in intensity.

TABLE 1: Locations and Notations of the Prominent Vibronic Bands in the Fluorescence Spectra of AN, PH, and PY

compound	location (nm)	notation
AN	376	A1
	398	A2
	423	A3
	448	A4
PH	346	H1
	356	H2
	363	H3
	383	H4
	406	H5
PY	365	Y0
	372	Y1
	378	Y2
	383	Y3
	388	Y4
	392	Y5

First, we discuss the synchronous correlation map (Figure 3a). By referring to Figure 1, the peak at 347 nm (H1) can be safely assignable to PH. The peaks at 356 nm (H2), 363 nm (H3), and 385 nm (H4) have positive correlation with H1, and thus are assigned to PH. On the other hand, the peaks at 377 nm (A1), 398 nm (A2), 422 nm (A3), and 448 nm (A4) have negative correlation with H1, and are assigned to AN. Also, there is positive correlation between the peaks H*i* and H*j*, and between the peaks A*i* and A*j*, while there is negative correlation between the peaks H*i* and A*j*. These results are self-consistent, and support the above peak assignments.

Next, we examine the asynchronous spectrum (Figure 3b). It is expected that asynchronous cross-peaks do not appear between the bands of the same probe because the intensities of these bands seem to change synchronously. This is confirmed by the fact that there are no asynchronous cross-peaks between the bands H*i* and H*j*, and between the bands A*i* and A*j* in Figure 3b. The intensity variation of the fluorescence bands in the present system is simply brought about by a change in concentration. There seem to be no specific interactions between the two probes and between the probe and solvent, because the concentrations of the probes are low, and the probes and solvent are nonpolar. These may be the reasons the fluorescence bands of the same probe change synchronously in their intensities, resulting in the absence of asynchronous cross-peaks between the bands H*i* and H*j*, and between the bands A*i* and A*j*.

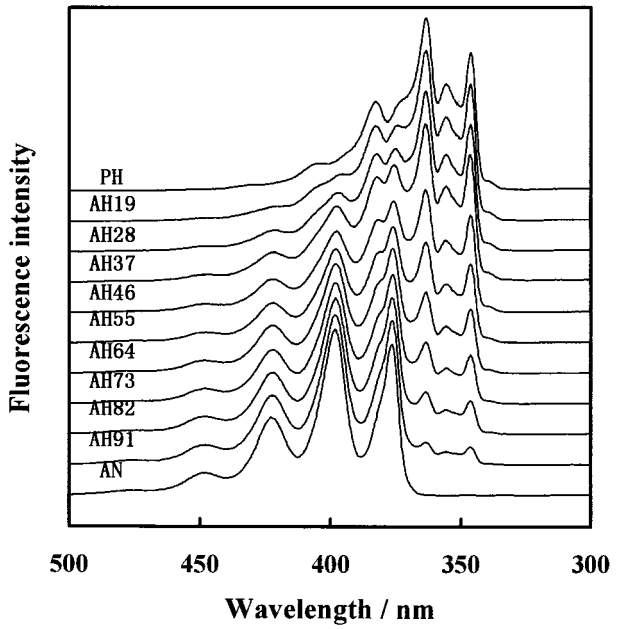

Figure 2. Fluorescence spectra of the mixtures of AN and PH with varying concentrations in cyclohexane solutions. The samples are excited at 262 nm. Excitation and emission band-passes are 5 and 3 nm, respectively. The symbols AH*mn* (*m*, *n* = 1−9) denote that the concentrations of AN and PH are *m* and *n* μM, respectively. For example, the symbol AH19 means that the sample contains AN and PH at the concentrations of 1 and 9 μM, respectively. The top and bottom spectra indicated by PH and AN, respectively, correspond to the samples which contain only PH or AN at the level of 10 μM.

It will be of value to note general features of fluorescence spectra. Fluorescence spectra usually consist of *progressions* of bands. The progression is defined as a series of vibronic bands which originate from $v' \rightarrow v''$ vibrational transitions ($v' = 0$ according to Kasha's rule,[36] and $v'' = 0, 1, 2, 3, ...$) associated with an electronic transition from the first excited singlet (S_1) to the ground (S_0) states. Here, the symbols v' and v'' denote vibrational quantum numbers of some active mode in S_1 and S_0 states, respectively. Because the bands in one progression belong to one vibrational mode, they seem to be affected to the same extent by intermolecular interactions including solute−solute interaction. Accordingly, it is probable that the members in the same progression change synchronously in their intensities when the composition of a solution is altered. This feature is in contrast to that of IR spectra. IR spectra consist of fundamental and combination bands of various vibrational modes which have different sensitivity to intermolecular interactions. Therefore, it sometimes occurs that each of the IR bands responds to a different extent to the intermolecular interactions such as hydrogen bonding.

In the present system, there should also be no cross-peaks between the bands H*i* and A*j*, if the signal intensities of PH and AN change linearly (and thus synchronously) with concentrations as indicated by eqs 1 and 2. Therefore, it is quite surprising that there are clear cross-peaks between the bands H*i* and A*j* in Figure 3b. There seem to be four possibilities for the cause of the presence of cross-peaks between the bands H*i*

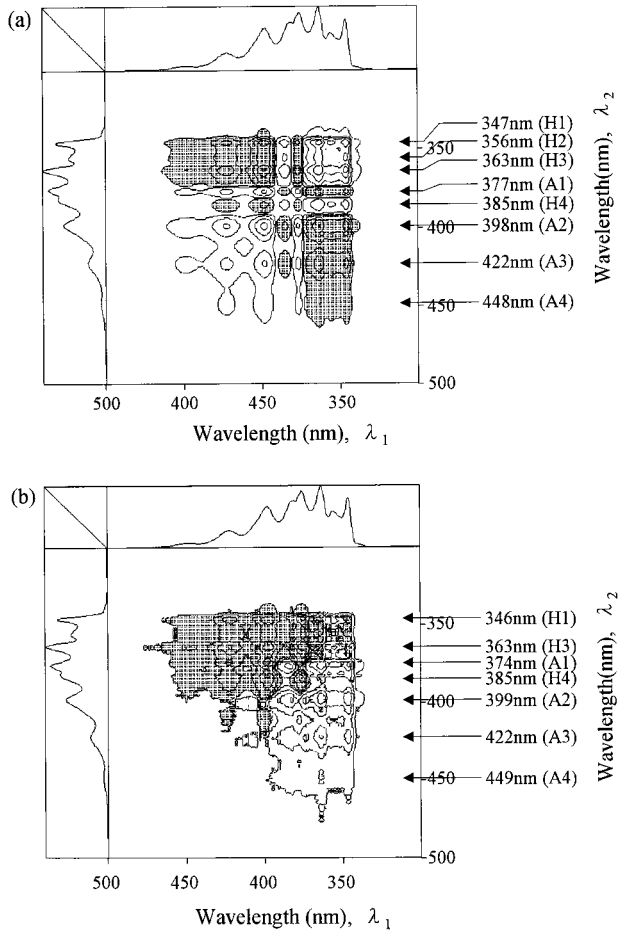

Figure 3. Synchronous (a) and asynchronous (b) 2D fluorescence correlation spectra of the mixtures of AN and PH in cyclohexane solutions, constructed from the spectra of Figure 2.

and A*j* (i.e., the cause of nonlinear intensity change of these fluorescence bands): (1) reabsorption of fluorescence, (2) *non*radiative energy transfer from PH to AN, (3) radiative energy transfer from PH to AN, and (4) inner filter effect.[23] In the reabsorption process, only the fluorescence bands at shorter wavelength (e.g. the bands A1 for AN and H1 for PH) are affected because these bands are overlapped with the $S_1 \leftarrow S_0$ absorption bands. As seen from Figure 3b, not only the A1 and H1 bands but also the other bands of AN and PH contribute to the appearance of asynchronous cross-peaks. Therefore, the possibility of reabsorption can be safely ruled out. In nonradiative energy transfer, the fluorescence of donor (PH) is quenched in concommitance with the enhancement of the fluorescence of acceptor (AN). It turned out that the fluorescence of PH is not quenched, nor is the fluorescence of AN enhanced in the mixed solutions. Thus, we exclude the possibility of the nonradiative energy transfer. Radiative energy transfer is an event in which the emitted fluorescence of the donor is absorbed by the acceptor. The overlap between the fluorescence spectrum of the donor and the absorption spectrum of the acceptor is important in this process, and the overlapped part of the fluorescence spectrum of the donor is reduced in intensity. This is in contrast to the feature of nonradiative energy transfer in which all spectral regions of the donor fluorescence are reduced in intensity. By referring to the absorption spectrum of AN, we realize that almost all parts of the PH fluorescence are overlapped with the strong $S_1 \leftarrow S_0$ absorption of AN. Accordingly, the radiative energy transfer can cause the appearance of asynchronous cross-peaks; i.e., can cause the

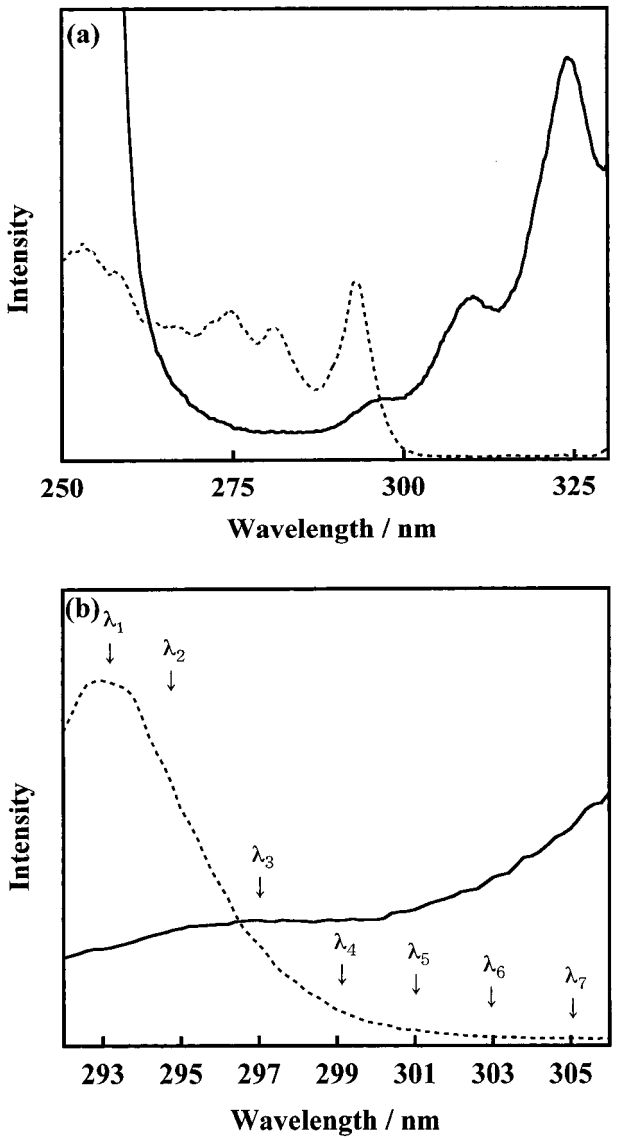

Figure 4. (a) Excitation spectra of AN (—) and PH (···) in cyclohexane solutions. (b) Expanded trace of Figure 4a. Concentrations: [AN] = 10 μM, [PH] = 10 μM. The fluorescence is monitored at 398 nm for AN and 363 nm for PH. Excitation and emission band-passes are 1.5 and 5 nm, respectively.

breakdown of the linear relationship given by eq 1. Another cause may be an inner filter effect. The samples were excited at 262 nm, where both AN and PH have significant absorption of light. Therefore, PH acts as an optical filter for excitation of AN, and vice versa. As PH concentration was decreased with increase in AN concentration (Figure 2), the AN fluorescence intensity was increased more rapidly than the increase in its concentration. This is also true for the change in the fluorescence intensity of PH. Consequently, a linear relationship between the fluorescence intensities of the probes and their concentrations can be broken down. At present, it is unclear which of the two mechanisms, radiative energy transfer and inner filter effect, dominantly operates for the appearance of asynchronous cross-peaks. However, it is clear that we should be careful about these effects when we interpret asynchronous maps in 2D fluorescence correlation analysis.

Figure 4a represents excitation spectra of AN and PH obtained for respective solutions. The spectra were observed by monitoring fluorescence intensities at fixed wavelengths (398 nm for AN and 363 nm for PH) while varying excitation wavelength

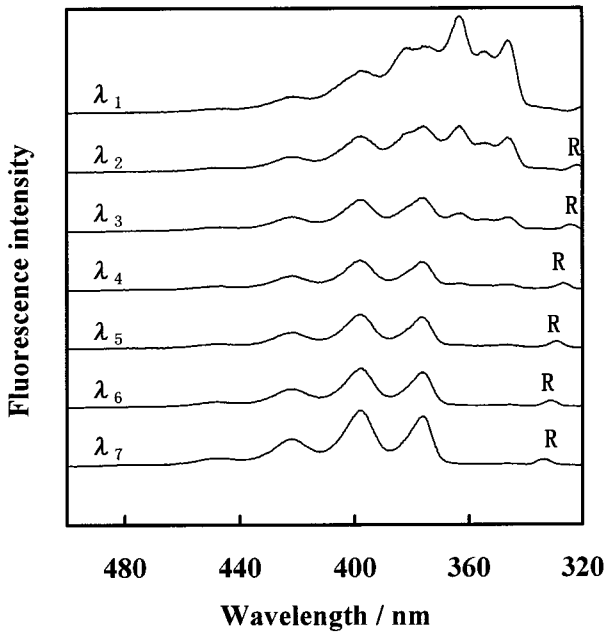

Figure 5. Fluorescence spectra of the mixtures of AN and PH excited at a series of wavelengths in a cyclohexane solution. Concentrations: [AN] = 5 μM, [PH] = 5 μM. Excitation and emission band-passes are 1.5 and 5 nm, respectively. Excitation wavelengths: $\lambda_1 = 293$ nm; $\lambda_2 = 295$ nm; $\lambda_3 = 297$ nm; $\lambda_4 = 299$ nm; $\lambda_5 = 301$ nm; $\lambda_6 = 303$ nm; $\lambda_7 = 305$ nm.

from 250 to 330 nm. The excitation spectra of both AN and PH, respectively, almost coincide with their absorption spectra. Figure 4b is an expansion of the 292−306 nm region of Figure 4a. Note that the intensity of AN fluorescence is increased with change of excitation wavelength from 293 nm (λ_1) to 305 nm (λ_7), whereas the intensity of PH fluorescence is decreased. Thus, we can bring about an intensity change in the fluorescence of AN and PH by varying excitation wavelength (*excitation perturbation*). In Figure 5, we show a series of the fluorescence spectra of a 1:1 mixture of AN and PH (5 μM for each) in a cyclohexane solution, which were obtained by varying the excitation wavelength. The symbols λ_i ($i = 1-7$) in Figure 5 indicate the excitation wavelengths, and correspond to those in Figure 4b. The band at the shortest wavelength, denoted R, is a Raman band of the solvent. As we expected, the spectra obtained by exciting the sample with λ_1 and λ_2 are dominated by PH fluorescence. By varying excitation light from λ_3 to λ_7, the spectra become gradually dominated by AN fluorescence.

Using a series of the fluorescence spectra in Figure 5, we calculated synchronous and asynchronous maps (Figure 6). In Figure 6a, the peaks at 347 nm (H1), 354 nm (H2), and 363 nm (H3) are assigned to PH because it is clear from Figure 1 that there are no bands of AN in this region. The peak at 383 nm (H4) has positive correlation with H1, and thus is assigned to PH. On the other hand, the peak at 422 nm (A3) has negative correlation with H1 and H3, and is assigned to AN. Note that the other bands of AN (i.e., A1, A2, and A4) are not generated in Figure 6b. The absence of these AN bands seems to be ascribed to the fact that the intensity of AN fluorescence is not much changed by varying excitation wavelength in the $\lambda_1 - \lambda_7$ region (see Figure 4b).

In the asynchronous correlation map (Figure 6b), there are cross-peaks between A*i* and H*j*. The appearance of the cross-peaks is attributed to the fact that the fluorescence intensities of AN and PH do not simultaneously change with each other, as seen in Figure 4b. The asynchronous correlation map is also

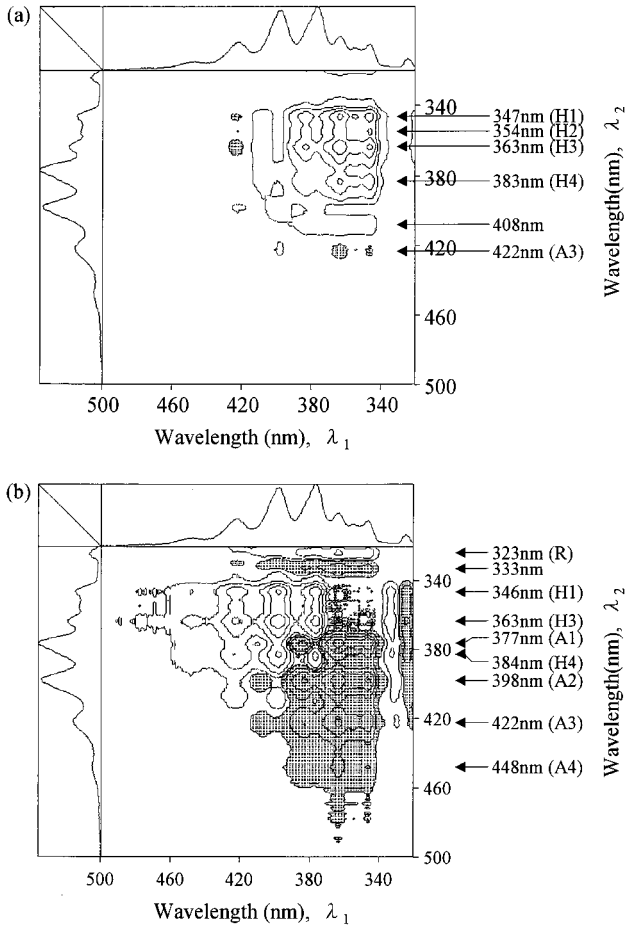

Figure 6. Synchronous (a) and asynchronous (b) 2D fluorescence correlation spectra of the mixtures of AN and PH in a cyclohexane solution, constructed from the spectra of Figure 5.

useful for assigning the bands in a manner similar to the case of Figure 3b.

4.2. Anthracene−Pyrene Mixture. The AN−PY pair was examined as a case where the fluorescence spectra are heavily overlapped, so that the band analysis is much more difficult by a conventional one-dimensional method. Figure 7 represents fluorescence spectra of AN and PY observed separately in cyclohexane solutions. The bands are denoted A*i* ($i = 1-4$) for AN and Y*i* ($i = 0-5$) for PY. As seen in Figure 7, the fluorescence spectra of AN and PY are heavily overlapped; only the band Y0 of PY is not overlapped with the bands of AN. The band Y0 is a hot band which originates from a vibrationally excited state ($\nu' = 1$) of the first excited singlet state (S_1) of PY. The locations of the PY bands are listed in Table 1.

In Figure 8 we show fluorescence spectra of the mixtures of AN and PY in cyclohexane solutions. It is noted that the spectra for the samples with nearly equimolar concentrations of AN and PY (i.e., AY46, AY55, and AY64) are extremely tangled by heavy overlap of the component spectra. To analyze the tangled spectra, we generated synchronous and asynchronous maps for the system using all spectra in Figure 8. The results are depicted in Figure 9.

In the synchronous correlation map (Figure 9a), the band at 365 nm (Y0) can be safely assigned to PY, because this band is clearly separated from others as seen from Figure 7. The band at 372 nm (Y1) is assigned to PY because this band has positive correlation with Y0. These two bands are used as clues for further assignment. The peaks at 383 nm (Y3), 388 nm (Y4), 392 nm (Y5), and 412 nm have positive correlation with Y1,

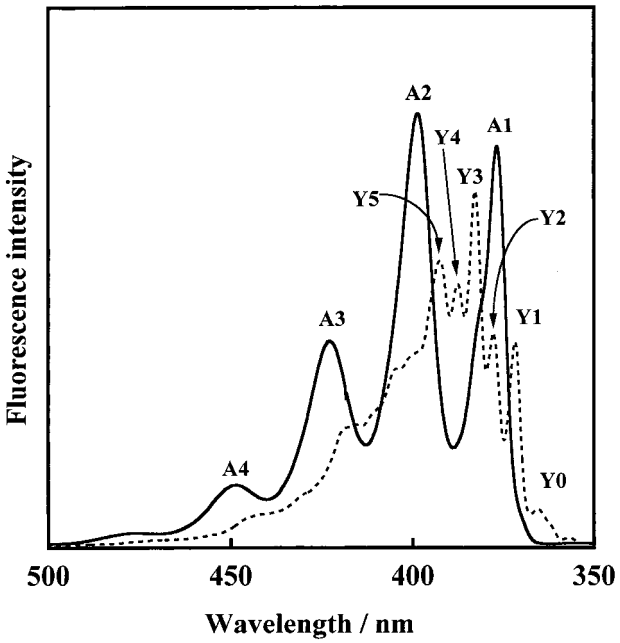

Figure 7. Fluorescence spectra of AN (—) and PY (···) in cyclohexane solutions. Concentrations: [AN] = 10 μM, [PY] = 10 μM. The samples are excited at 321 nm. Excitation and emission band-passes are 10 and 1.5 nm, respectively. The excitation wavelength, 321 nm, is selected in order that the fluorescence of both probes may become comparable in intensity.

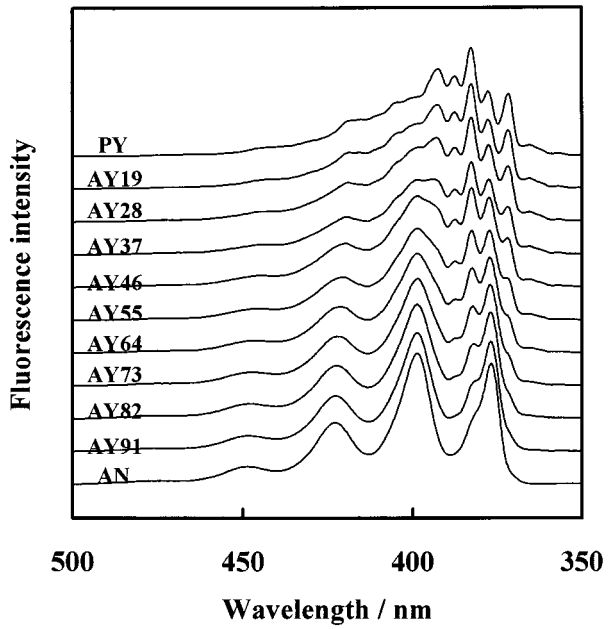

Figure 8. Fluorescence spectra of the mixtures of AN and PY with varying concentrations in cyclohexane solutions. The samples are excited at 321 nm. Excitation and emission band-passes are 10 and 1.5 nm, respectively. The symbols AY*mn* (*m*, *n* = 1−9) denote that the concentrations of AN and PY are *m* and *n* μM, respectively. The top and bottom spectra indicated by PY and AN, respectively, correspond to the samples which contain only PY or AN at the level of 10 μM.

and thus are assigned to PY. The peak at 412 nm corresponds to the band which appears as a shoulder of the Y5 band (Figure 7). Although the band at 412 nm is indistinct in the original spectra (Figure 8), it is clearly displayed in the 2D correlation map. This is one of the examples which demonstrate the advantage of the 2D correlation method. The peaks at 376 nm (A1), 399 nm (A2), 424 nm (A3), and 451 nm (A4) have

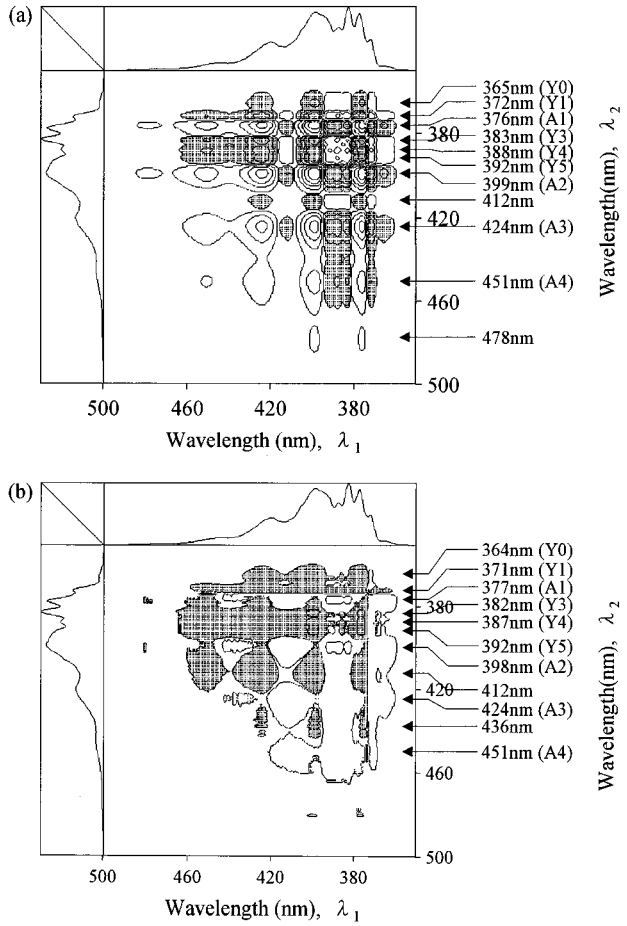

Figure 9. Synchronous (a) and asynchronous (b) 2D fluorescence correlation spectra of the mixtures of AN and PY in cyclohexane solutions, constructed from the spectra of Figure 8.

negative correlation with Y1, and thus are assigned to AN. Furthermore, if we take an overview of the synchronous correlation map, there is positive correlation between the peaks Y*i* and Y*j*, and between the peaks A*i* and A*j*, while there is negative correlation between the peaks Y*i* and A*j*. These results are self-consistent.

There are cross-peaks between the AN and PY bands in the asynchronous correlation map (Figure 9b), whereas no cross-peaks appear between the bands of the same probe. This feature gives additional support for the band assignment based on the synchronous correlation map. The presence of the asynchronous cross-peaks between the AN and PY bands can be discussed in a similar way to that in the AN−PH case.

Figure 10a shows excitation spectra of AN and PY obtained for individual solutions. The spectrum of AN was observed under the same conditions as in Figure 4. The spectrum of PY was obtained by monitoring fluorescence intensity at 382 nm. The excitation spectra of both AN and PY are almost identical to their respective absorption spectra. The absorption of PY ranging from 300 to 340 nm is assigned to the $S_2 \leftarrow S_0$ transition and that from 250 to 280 nm is assigned to the $S_3 \leftarrow S_0$ transition. The $S_1 \leftarrow S_0$ transition is located in the region from 350 to 370 nm. However, this transition is forbidden and the bands appear as a shoulder of the strong $S_2 \leftarrow S_0$ transition. This is the reason for the breakdown of mirror-image symmetry between the absorption and fluorescence spectra of PY.

In contrast to the AN−PH system, it is difficult to find a wide spectral region for the AN−PY system where the AN absorption monotonically increases (or decreases) while the PY

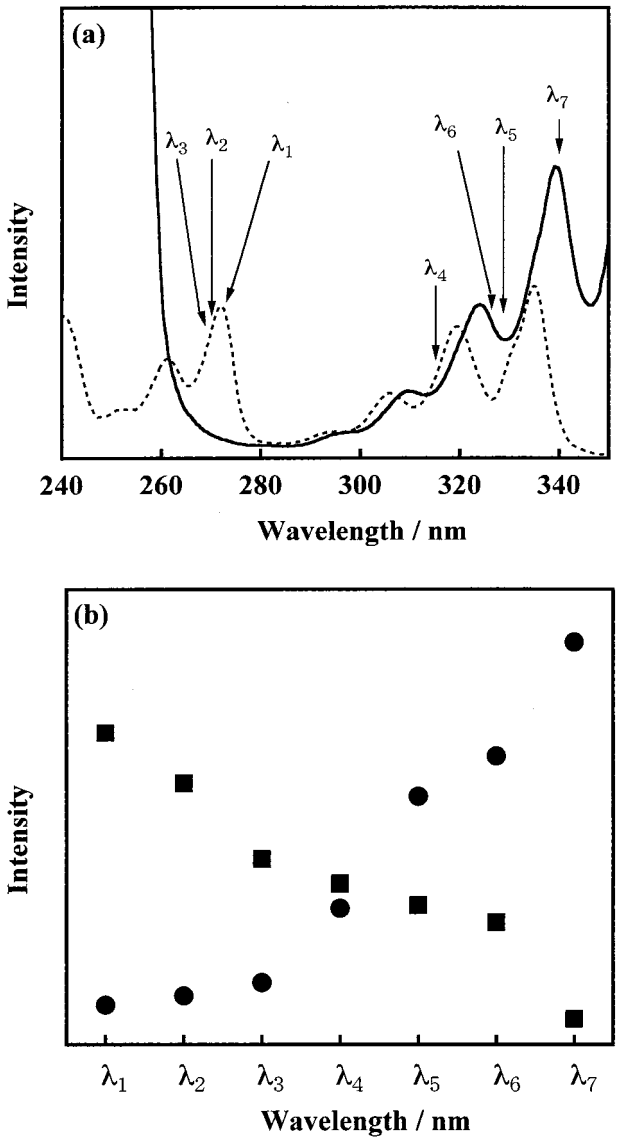

Figure 10. (a) Excitation spectra of AN (—) and PY (···) in cyclohexane solutions. (b) Dependence of the fluorescence intensities of AN (●) and PY (■) on the excitation wavelength. Concentrations: [AN] = 10 μM, [PY] = 10 μM. The fluorescence is monitored at 398 nm for AN and 382 nm for PY. Excitation and emission band-passes are 1.5 and 5 nm, respectively. Excitation wavelengths: $\lambda_1 = 272$ nm; $\lambda_2 = 270$ nm; $\lambda_3 = 268$ nm; $\lambda_4 = 315$ nm; $\lambda_5 = 328$ nm; $\lambda_6 = 326$ nm; $\lambda_7 = 343$ nm.

absorption decreases (or increases). Therefore, we picked the excitation wavelengths ($\lambda_1 - \lambda_7$) from several discrete spectral regions as shown in Figure 10a (cf. Figure 4b for the AN−PH system). The fluorescence intensities of AN and PY are plotted against the excitation wavelength in Figure 10b. The intensity of AN fluorescence increases with the change of excitation wavelength from λ_1 to λ_7, whereas the intensity of PY fluorescence decreases. In Figure 11, we show a series of fluorescence spectra of a 1:1 mixture of AN and PY (5 μM for each) in a cyclohexane solution, which were obtained by varying the excitation wavelength from λ_1 to λ_7. As expected, the top two spectra are dominated by PY fluorescence, and the bottom two spectra are dominated by AN fluorescence. The middle three spectra are extremely tangled by heavy overlap of the component spectra which have comparable intensities.

Using a series of the fluorescence spectra in Figure 11, we calculated synchronous and asynchronous maps (Figure 12). In contrast to the case of excitation perturbation for an AN−PH

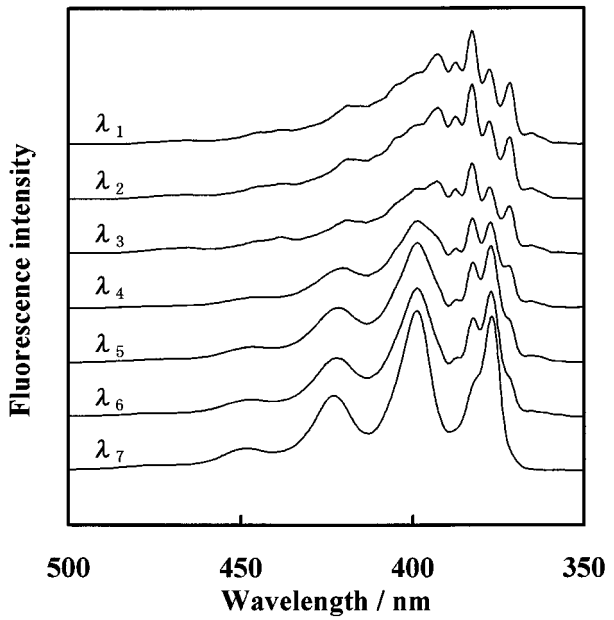

Figure 11. Fluorescence spectra of the mixtures of AN and PY excited at various wavelengths in a cyclohexane solution. Concentrations: [AN] = 5 μM, [PY] = 5 μM. Excitation and emission band-passes are 1.5 and 5 nm, respectively. Excitation wavelengths are indicated by λ_i (i = 1−7), and are the same as those in Figure 10.

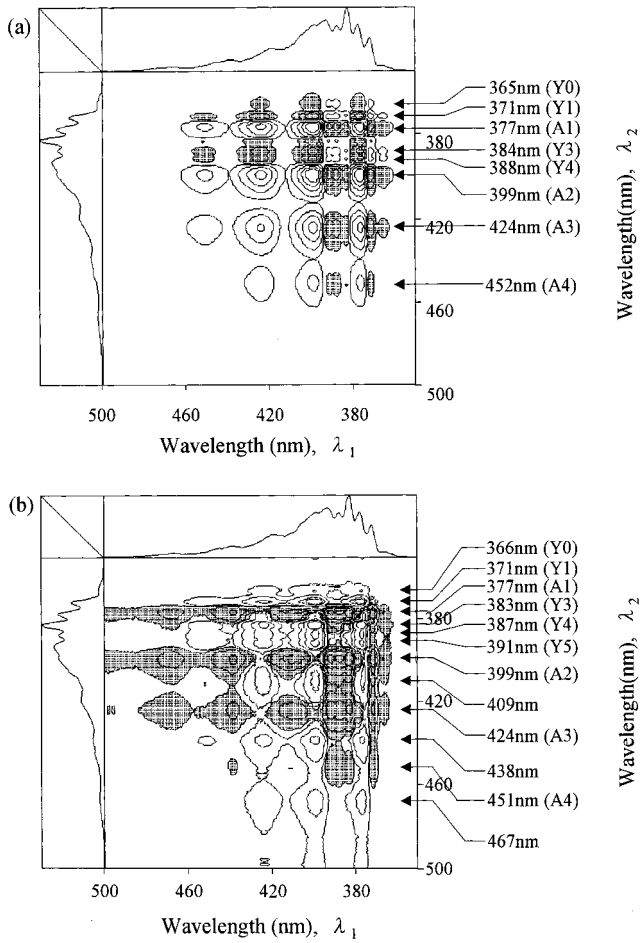

Figure 12. Synchronous (a) and asynchronous (b) 2D fluorescence correlation spectra of the mixtures of AN and PY in a cyclohexane solution, constructed from the spectra of Figure 11.

system (Figure 6a), there are many auto- and cross-peaks in the synchronous correlation map (Figure 12a). This seems to

be because the fluorescence intensities of both AN and PY are considerably changed by varying the excitation wavelength from λ_1 to λ_7 (see Figure 10). In Figure 12a, it is obvious that the peak at 365 nm (Y0) arises from the hot band of PY. The band at 371 nm (Y1) is assigned to PY because this band has positive correlation with Y0. The peaks at 384 nm (Y3) and 388 nm (Y4) have positive correlation with Y1, and thus are assigned to PY. The peaks at 377 nm (A1), 399 nm (A2), 424 nm (A3), and 452 nm (A4) have negative correlation with Y1, and thus are assigned to AN. As in the case of concentration perturbation, there is positive correlation between the peaks Y*i* and Y*j*, and between the peaks A*i* and A*j*, while there is negative correlation between the peaks H*i* and A*j*. These results support the above peak assignments.

There are many cross-peaks in the asynchronous correlation map (Figure 12b). As already discussed, the asynchronous cross-peaks appear only between the bands for different compounds. Therefore, the asynchronous correlation map is useful for confirming the band assignment based on the synchronous correlation map. Note that there are distinct bands at 409, 438, and 467 nm which have asynchronous correlation with the A2 band. According to the previous discussion, these bands can be assigned to PY. The assignment for the band at 409 nm is also supported by the fact that this band corresponds to the band at 412 nm in Figure 9a. It is remarkable that we could clearly detect these three PY bands in the 2D correlation maps, although they appear as obscure bands in the original one-dimensional spectrum. This demonstrates the usefulness of 2D correlation method in fluorescence spectroscopy.

5. Concluding Remarks

In this paper we have tried to extend 2D correlation technique to the field of fluorescence spectroscopy. The fluorescence compounds examined were AN, PH, and PY, which are commonly used fluorescence probes employed widely in solutions, colloids, and solid systems.[23−25] The perturbation modes for causing fluorescence intensity changes are concentration change (concentration perturbation) and excitation-wavelength change (excitation perturbation). Both perturbation methods could give a series of perturbed spectra, which led to the development of clear synchronous and asynchronous maps. The 2D correlation maps thus obtained were used to analyze the complicated fluorescence spectra of the mixture of the probes.

Several advantages of the 2D correlation method in fluorescence spectroscopy have emerged from this study. First, almost all bands in the extremely tangled fluorescence spectra of the mixture of the AN−PH pair and of the AN−PY pair could be safely assigned.[37] Such assignments are impossible by the conventional one-dimensional method. Second, weak bands could be clearly detected by the 2D correlation methods. For example, the PY band at 412 nm appears as a shoulder of the strong band at 392 nm, so that this band is indistinct in the original one-dimensional spectra (Figures 7 and 8). However, the PY band at 412 nm is distinctly shown in the 2D synchronous correlation map (Figure 9a). Another example can be seen in the PY bands at 438 and 467 nm. Although they appear as obscure shoulder bands in the original one-dimensional spectrum (Figure 7), they are clearly displayed in the 2D asynchronous correlation map (Figure 12b).

As stated in the Introduction section, there are other ways to bring about intensity changes in fluorescence spectra. Quenching and sensitization, for example, seem to be of great use as perturbation techniques. Investigations using such approaches are now in progress.

References and Notes

(1) Noda, I. *Bull. Am. Phys. Soc*. **1986**, *31*, 520.
(2) Noda, I. *J. Am. Chem. Soc*. **1989**, *111*, 8116.
(3) Noda, I. *Appl. Spectrosc*. **1990**, *44*, 550.
(4) Noda, I. *Appl. Spectrosc*. **1993**, *47*, 1329.
(5) Czarnecki, M. A. *Appl. Spectrosc*. **1998**, *52*, 1583.
(6) Magtoto, N. P.; Sefara, N. L.; Richardson, H. H. *Appl. Spectrosc*. **1999**, *53*, 178.
(7) Nabet, A.; Pezolet, M. *Appl. Spectrosc*. **1997**, *51*, 466.
(8) Noda, I.; Liu, Y.; Ozaki, Y. *J. Phys. Chem*. **1996**, *100*, 8665.
(9) Muller, M.; Buchet, R.; Fringeli, U. P. *J. Phys. Chem*. **1996**, *100*, 10810.
(10) Jiang, E. Y.; McCarthy, W. J.; Drapcho, D. L.; Crocombe, R. A. *Appl. Spectrosc*. **1997**, *51*, 1736.
(11) Ozaki, Y.; Noda, I. *J. NIR Spectrosc*. **1996**, *4*, 85.
(12) Noda, I.; Liu, Y.; Ozaki, Y.; Czarnecki, M. A. *J. Phys. Chem*. **1995**, *99*, 3068.
(13) Sefara, N. L.; Magtoto, N. P.; Richardson, H. H. *Appl. Spectrosc*. **1997**, *51*, 536.
(14) Liu, Y.; Ozaki, Y.; Noda, I. *J. Phys. Chem*. **1996**, *100*, 7326.
(15) Ozaki, Y.; Liu, Y.; Noda, I. *Macromolecules* **1997**, *30*, 2391.
(16) Ozaki, Y.; Liu, Y.; Noda, I. *Appl. Spectrosc*. **1997**, *51*, 526.
(17) Czarnecki, M. A.; Maeda, H.; Ozaki, Y.; Suzuki, M.; Iwahashi, M. *J. Phys. Chem. A* **1998**, *102*, 9117.
(18) Wang, Y.; Murayama, K.; Myojo, Y.; Tsenkova, R.; Hayashi, N.; Ozaki, Y. *J. Phys. Chem. B* **1998**, *102*, 6655.
(19) Noda, I.; Liu, Y.; Ozaki, Y. *J. Phys. Chem*. **1996**, *100*, 8674.
(20) Schultz, C. P.; Fabian, H.; Mantsch, H. H. *Biospectroscopy* **1998**, *4*, 19.
(21) Ren, Y.; Ozaki, Y.; Murakami, T.; Nishioka, T.; Nakashima, K. *Macromol. Symp*. **1999**, *141*, 167.
(22) Ren, Y.; Murakami, T.; Nishioka, T.; Nakashima, K.; Noda, I.; Ozaki, Y. *Macromolecules* **1999**, *32*, 6307.
(23) Lakowicz, J. R. *Principles of Fluorescence Spectroscopy*; Plenum: New York, 1986.
(24) Kalyanasundaram, K. *Photochemistry in Microheterogeneous Systems*; Academic Press Inc.: New York, 1987.
(25) Guillet, J. E. *Polymer Photophysics and Photochemistry*; Cambridge University Press: Cambridge, 1985.
(26) Esteves da Silva, J. C. G.; Machado, A. A. S. C.; Silva, C. S. P. C. O. *Anal. Chim. Acta*. **1996**, *318*, 365.
(27) Esteves da Silva, J. C. G.; Machado, A. A. S. C. *Analyst* **1997**, *122*, 1299.
(28) Roch, T. *Anal. Chim. Acta*. **1997**, *356*, 61.
(29) Siegel, J. A. *Anal. Chem*. **1985**, *57*, 934A.
(30) Beltran, J. L.; Ferrer, R.; Guiteras, J. *Anal. Chim. Acta*. **1998**, *373*, 311.
(31) Jacobson, M. P.; Coy, S. L.; Field, R. W. *J. Chem. Phys*. **1997**, *107*, 8349.
(32) Coy, S. L.; Jacobson, M. P.; Field, R. W. *J. Chem. Phys*. **1997**, *107*, 8357.
(33) O'Brien, J. P.; Jacobson, M. P.; Sokol, J. J.; Coy, S. L.; Field, R. W. *J. Chem. Phys*. **1998**, *108*, 7100.
(34) Roselli, C.; Burie, J.-R.; Mattioli, T.; Boussac, A. *Biospectroscopy* **1995**, *1*, 329.
(35) Nakashima, K.; Ren, Y.; Nishioka, T.; Tsubahara, N.; Noda, I.; Ozaki, Y. *J. Phys. Chem. B* **1999**, *32*, 6704.
(36) Kasha, M. *Discuss. Faraday Soc*. **1950**, *9*, 14.
(37) One may wonder if the 2D correlation analysis has a potential difficulty when applied to the spectra comprised of broad and highly overlapped bands. Such difficulty may seem especially serious in the application to fluorescence spectra. However, the present 2D fluorescence correlation approach clearly shows its success in analyzing spectra which consist of highly overlapped bands. Similar successful analysis of broad and highly overlapped band systems by the 2D correlation technique has also been shown in 2D NIR studies.[11−22]